

Systematic reduction of sign errors in many-body calculations of atoms and molecules

Michal Bajdich,¹ Murilo L. Tiago,¹ Randolph Q. Hood,² Paul R. C. Kent,³ and Fernando A. Reboredo¹

¹*Materials Science and Technology Division, Oak Ridge National Laboratory, Oak Ridge, TN 37831, USA*

²*Lawrence Livermore National Laboratory, Livermore, CA 94550, USA*

³*Center for Nanophase Materials Sciences, Oak Ridge National Laboratory, Oak Ridge, TN 37831, USA*

(Dated: April 15, 2010)

The self-healing diffusion Monte Carlo algorithm (SHDMC) [Phys. Rev. B **79**, 195117 (2009), *ibid.* **80**, 125110 (2009)] is shown to be an accurate and robust method for calculating the ground-state of atoms and molecules. By direct comparison with accurate configuration interaction results for the oxygen atom we show that SHDMC converges systematically towards the ground-state wave function. We present results for the challenging N₂ molecule, where the binding energies obtained via both energy minimization and SHDMC are near chemical accuracy (1 kcal/mol). Moreover, we demonstrate that SHDMC is robust enough to find the nodal surface for systems at least as large as C₂₀ starting from random coefficients. SHDMC is a linear-scaling method, in the degrees of freedom of the nodes, that systematically reduces the fermion sign problem.

PACS numbers: 02.70.Ss, 02.70.Tt

Since electrons are fermions, their many-body wave functions must change sign when the coordinates of any pair are interchanged. In contrast, the sign of a bosonic wave functions is unchanged for any coordinate interchange. Due to this misleadingly small difference, the ground-state energy of bosons can be determined by quantum Monte Carlo (QMC) methods [1, 2] with an accuracy limited only by computing time, while QMC calculations of fermions are either exponentially difficult, or are stabilized by imposing a systematic error, a direct consequence of our lack of knowledge of the fermionic nodal surface. Therefore, one of the most important problems in many-body electronic structure theory is to accurately find representations of the fermion nodes [3, 4], the locations where the fermionic wave function changes sign, the so-called “fermion sign problem”.

The sign problem limits (i) the number of physical systems where *ab initio* QMC can be applied and (ii) our ability to improve approximations of density functional theory (DFT) using QMC results [5]. More importantly, it limits our overall understanding of the effects of interactions in fermionic systems. Therefore, a method to circumvent the sign problem with reduced computational cost could transform Condensed Matter Theory, Quantum Chemistry and Nuclear Physics among other fields.

Arguably the most accurate technique for calculating the ground-state of a many-body system with more than 20 fermions is diffusion Monte Carlo (DMC). The standard DMC algorithm [5] finds the lowest energy of all wave functions that share the nodal surface $S_T(\mathbf{R})$ imposed by a trial wave function $\Psi_T(\mathbf{R})$. This is the fixed-node approximation where the resultant energy E_{DMC} is a rigorous upper bound of the exact ground-state energy [6, 7]. The exact ground-state energy is obtained only when $\Psi_T(\mathbf{R})$ has the same nodal surface as the exact ground-state wave function.

If the exact nodes are not provided, the implicit fixed-node ground-state wave function $\Psi_{FN}(\mathbf{R})$ will exhibit discontinuities in its gradient [7, 8] (i.e. kinks) on some parts of $S_T(\mathbf{R})$. We recently proved [8] that by locally smoothing these dis-

continuities in $\Psi_{FN}(\mathbf{R})$, a new trial wave function can be obtained with improved nodes. This proof enables an algorithm that systematically moves the nodal surface $S_T(\mathbf{R})$ towards the one of an eigen-state. If the form of trial wave function is sufficiently flexible, and given sufficient statistics, this process leads to an exact eigen-state wave function [8, 9]. We named the method self-healing DMC (SHDMC), since the trial wave function is self-corrected in DMC and can recover even from a poor starting point.

In this Letter, we report the first applications of SHDMC to real atoms and molecules (O, N₂, C₂₀). SHDMC energies are within error bars of DMC calculations using the current state of the art approach [10, 11]. Tests of SHDMC for C₂₀ demonstrate that our method can be applied at the nanoscale. Its cost scales linearly with the number of independent degrees of freedom of the nodes with an accuracy limited only by the achievable statistics and choice of representation of the nodes.

Brief review of SHDMC — SHDMC is fundamentally different from optimization methods used in variational Monte Carlo (VMC): [1, 2] (i) the wave function is directly optimized based on a property of the nodal surface and not on the local energy or its variance, and (ii) the nodes are optimized at the DMC level (as opposed to a VMC based algorithm).

Using a short-time many-body propagator, SHDMC samples the coefficients of an improved wave function removing the artificial derivative discontinuities of $\Psi_{FN}(\mathbf{R})$ arising from the inexact nodes. Repeated application of this method results in the best nodal surface for a given basis. For wave functions expanded in a complete basis it can be shown that the final accuracy is limited only by the statistics [8, 9].

In SHDMC (see Refs. 8, 9 for details), the weighted walker distribution is [5]

$$\begin{aligned} f(\mathbf{R}, \tau' + \tau) &= \Psi_T^*(\mathbf{R}, \tau') \left[e^{-\tau(\hat{H}_{FN} - E_T)} \Psi_T(\mathbf{R}, \tau') \right] \quad (1) \\ &= \lim_{N_c \rightarrow \infty} \frac{1}{N_c} \sum_{i=1}^{N_c} W_i^j(k) \delta(\mathbf{R} - \mathbf{R}_i^j), \end{aligned}$$

where

$$\Psi_T(\mathbf{R}, \tau') = e^{J(\mathbf{R})} \sum_n^{\sim} \lambda_n(\tau') \Phi_n(\mathbf{R}) \quad (2)$$

is a trial function where \sum_n^{\sim} represents a truncated sum, $\{\Phi_n(\mathbf{R})\}$ forms a complete orthonormal basis of the antisymmetric Hilbert space and $e^{J(\mathbf{R})}$ is a symmetric Jastrow factor. In Eq. (1), $\hat{\mathcal{H}}_{FN}$ is the fixed-node Hamiltonian [$\hat{\mathcal{H}}_{FN}$ is the many-body Hamiltonian with an infinite potential at the nodes of $\Psi_T(\mathbf{R}, \tau')$] and E_T is an energy reference. Next, \mathbf{R}_i^j corresponds to the position of the walker i at step j of N_c equilibrated configurations. The weights $W_i^j(k)$ are given by

$$W_i^j(k) = e^{-[E_i^j(k) - E_T]\tau} \text{ with } E_i^j(k) = \frac{1}{k} \sum_{\ell=0}^{k-1} E_L(\mathbf{R}_i^{j-\ell}), \quad (3)$$

where E_T in Eq. (3) is periodically adjusted so that $\sum_i W_i^j(k) \approx N_c$ and τ is $k\delta\tau$ (with k being a number of steps and $\delta\tau$ a standard DMC time step).

From Eq. (1), one can formally obtain

$$\tilde{\Psi}_T(\mathbf{R}, \tau' + \tau) = f(\mathbf{R}, \tau' + \tau) / \Psi_T^*(\mathbf{R}, \tau'). \quad (4)$$

We now define the local smoothing function to be

$$\tilde{\delta}(\mathbf{R}', \mathbf{R}) = \sum_n^{\sim} e^{J(\mathbf{R}')} \Phi_n(\mathbf{R}') \Phi_n^*(\mathbf{R}) e^{-J(\mathbf{R})}. \quad (5)$$

Applying Eq. (5) to both sides of Eq. (4), using Eq. (1), and integrating over \mathbf{R} we obtain

$$\Psi_T(\mathbf{R}, \tau' + \tau) = e^{J(\mathbf{R})} \sum_n^{\sim} \lambda_n(\tau' + \tau) \Phi_n(\mathbf{R}), \quad (6)$$

with

$$\lambda_n(\tau' + \tau) = \lim_{N_c \rightarrow \infty} \frac{1}{\mathcal{N}} \sum_i^{N_c} W_i^j(k) e^{-2J(\mathbf{R}_i^j)} \frac{\Phi_n^*(\mathbf{R}_i^j)}{\Phi_T^*(\mathbf{R}_i^j, \tau')} \quad (7)$$

where $\mathcal{N} = \sum_{i=1}^{N_c} e^{-2J(\mathbf{R}_i^j)}$ normalizes the Jastrow factor. These new $\lambda_n(\tau' + \tau)$ [Eq. (7)] are used to construct a new trial wave function [Eq. (2)] recursively within DMC (therefore the name self-healing DMC). The weights in Eq. (3) can be evaluated within (i) a branching algorithm [8] for $\tau' \rightarrow \infty$ or (ii) a fixed population scheme for small τ' [9, 12]. The former method is more robust, but the latter improves final convergence. Equation (7) can be related to the maximum-overlap method used for bosonic wave functions [13].

Since SHDMC is targeted for large systems we report validations using pseudopotentials.

Validation of SHDMC with configuration interaction (CI) calculations for the O atom — In short, CI is the diagonalization of the many-body Hamiltonian in a truncated basis of Slater determinants. We chose to study the ^3P ground-state of the O atom because it has at least two valence electrons in

TABLE I: Total energies (and correlation % in $\{\}$) for the ground-state of O obtained with CI, coupled-cluster (CCSD(T) [15]) and SHDMC (no Jastrow). Other symbols defined in the text.

Method	VTZ		V5Z	
	N_b	E [Ha]{[%]}	N_b	E [Ha]{[%]}
CI ^a	775182	-15.88258{89.0}	1762377	-15.89557{95.7}
CCSD(T) ^b	-	-15.88204{88.8}	-	-15.90166{98.8}
SHDMC	539	-15.9003(2){98.1(1)}	1481	-15.9040(4){100.0(2)}

^afull-CI in VTZ and CISDTQ in V5Z.

^bfrom Ref. [14].

both spin channels [14]. The single-particle orbitals were expanded in VTZ and V5Z Gaussian basis sets [14] using the GAMESS [16] code. To facilitate a direct comparison between SHDMC and CI, no Jastrow factor was employed.

Figure 1 shows a direct comparison of the first 250 converged coefficients λ_n obtained using SHDMC with those from the largest CI calculation (see Table I). The initial SHDMC trial wave function was the Hartree–Fock (HF) solution, and the final SHDMC coefficients resulted from sampling the 1481 most significant excitations in the CI. We used $\delta\tau = 0.01 \text{ a.u.}$, $\tau = 0.5 \text{ a.u.}$, and 16 iterations of trial wave function projection ($\approx 6 \times 10^7$ sampled configurations).

Figure 1 shows the excellent agreement between the coefficients λ_n obtained independently by SHDMC and CI. A perfect agreement is guaranteed only in the limit of a complete basis and $N_c \rightarrow \infty$. The small differences in Fig. 1 are due to the truncation of the expansion and the stochastic error in λ_n . The inset shows the residual projection as a function of the total number N_b of CSFs included in the expansion, normalized either using the entire CI expansion (circles) or using a Ψ_{CI} that included only the λ_n sampled in SHDMC (squares). The residual projection is much smaller for the truncated norm than the full norm illustrating that most of the error in Ψ_{SHDMC} is from truncation and not limited statistics. Similar results were obtained for the C atom (not shown).

Validation with Energy Minimization for N_2 — We also compared the VMC and DMC energies of wave functions optimized with energy minimization in VMC (EMVMC) [10, 11] and SHDMC using the QWALK [18] code. EMVMC can be briefly described as a generalized CI with an additional Jastrow factor (sampling the Hamiltonian stochastically and solving a generalized eigenvalue problem). Several bases were obtained from series of complete active space (CAS) and restricted active space (RAS) [19] multiconfiguration self-consistent field (MCSCF) calculations [distributing 10 electrons into m active orbitals: CAS(10, m)]. We retained the N_b basis functions with coefficients of absolute value larger than a given cutoff. Subsequently, for each basis, we performed energy minimization of the Jastrow and the coefficients of trial wave function using a mixture of 95% of energy and 5% of variance. We also sampled these N_b coefficients in SHDMC recursively starting from HF solution. For a clear comparison

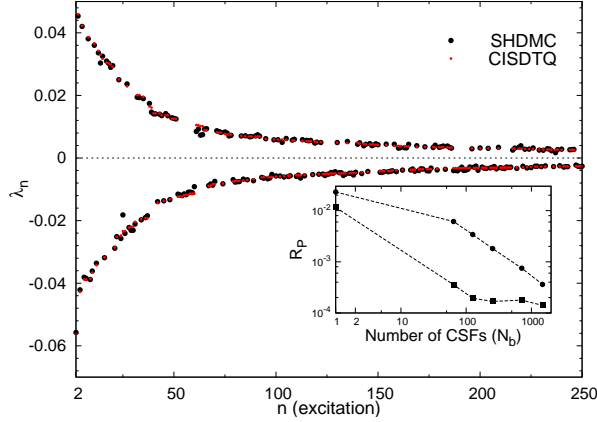


FIG. 1: Comparison of the values of the coefficients λ_n corresponding to the first 250 excitations of a converged SHDMC trial wave function (large black circles) with a large CISDTQ wave function (small red circles) for the oxygen atom. The first coefficient of the expansion, 0.9769, is not shown. Inset: Residual projection ($R_P = 1 - |\langle \Psi_{\text{SHDMC}} | \Psi_{\text{CI}} \rangle| / |\langle \Psi_{\text{CI}} | \Psi_{\text{CI}} \rangle|$) as a function of the number of CSFs included: circles R_P obtained with the full CISDTQ norm, squares R_P obtained with the truncated CISDTQ norm.

we used the same Jastrow in EMVMC and SHDMC.

We performed these calculations for the ground-state ($^1\Sigma_g^+$) of N_2 at the experimental geometry [20]. Figure 2 shows the resulting VMC and DMC energies obtained for wave functions optimized independently with EMVMC and SHDMC methods for the largest RAS(10,43) (2629447 CSFs yielding $E = -19.921717$) Slater-Jastrow wave function (See also Table II). In EMVMC, as previously observed for C_2 and Si_2 [11], we found a systematic reduction in the fixed-node errors, even when starting from the smallest CAS wave function (see Table II). When we compare with SHDMC optimized wave functions we find an excellent agreement in both VMC and DMC energies. Therefore, SHDMC improves the nodes systematically starting from the HF ground-state.

Since retaining all the determinants in the wave function would be costly, we performed calculations with different N_b to extrapolate (quadratically) the final energies as $\sum_n (\lambda_n^{\text{MCSCF}})^2 \rightarrow 1$ (see Fig. 2). The extrapolated DMC energies reached chemical accuracy (see also Table II).

Proof of principle in larger systems — Figures 1 and 2 show that SHDMC produces reliable and accurate results for small systems starting from the HF nodes. It is also important to demonstrate that SHDMC is a robust approach that can find the correct nodal surface topology of much larger systems even when starting from random nodal surfaces.

Figure 3 shows proof of principle results obtained for a C_{20} fullerene. These calculations used the branching SHDMC algorithm[8] implemented by us in CASINO [22]. Two electrons were removed from the system to obtain a non-interacting DFT ground-state wave function invariant under any transformation belonging to the icosahedral group (I_h) symmetry. The orbitals were obtained directly with the real

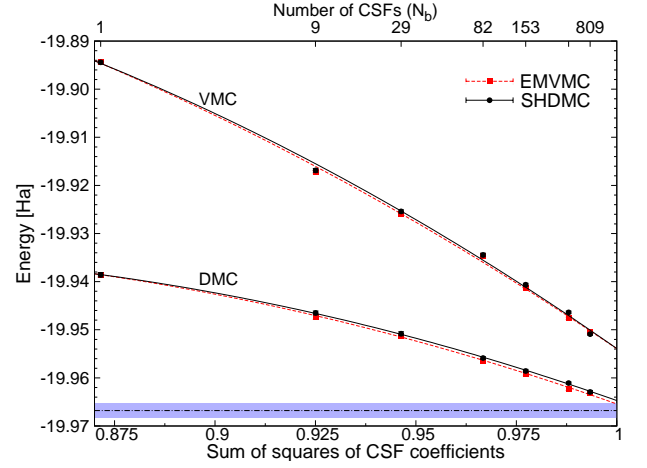


FIG. 2: Total energies obtained for N_2 with VMC and DMC methods for wave functions optimized via EMVMC [10] (squares) and SHDMC (circles) as a function of the square of the norm of the CI coefficients retained in the basis $[\sum_n (\lambda_n^{\text{MCSCF}})^2]$. The lines are parabolic extrapolations to 1. The dot-dashed line represents the scalar relativistic core-corrected estimate of the exact energy (see Table II). The shaded area is the region of chemical accuracy.

TABLE II: Comparison of total and binding DMC energies of N_2 for wave functions optimized with EMVMC and SHDMC for increasingly larger basis (see text). All SHDMC calculations started from the single HF determinant. Binding energies were obtained using an atomic energy^c of -9.80213(5) Ha, a core-correlations correction of 1.4 mHa [21], and a zero point energy of 5.4 mHa [20].

Wave function	Total energy [Ha]		Binding energy [eV]	
	EMVMC	SHDMC	EMVMC	SHDMC
1 determinant	-19.9362(5)		9.07(1)	
CAS(10,14)	-19.9536(6)	-19.9536(6)	9.54(2)	9.54(2)
RAS(10,35)	-19.9639(4)	-19.9627(4)	9.83(1)	9.79(1)
RAS(10,43)	-19.9654(4)	-19.9647(4)	9.87(1)	9.85(1)
Estimated exact	-19.9668(2) ^a		-9.900(1) ^b	

^aBased on the scalar relativistic core-corrected estimate from Ref. [21].

^bUsing the experimental value from Ref. [20].

^cBased on a large multi-determinant DMC calculation.

space code PARSEC [23] and classified according to their irreducible representations for I_h and its subgroup D_{2h} . For this calculation 694 excitations (determinants) were sampled. No CI prefiltering of determinants is required; we only use the selection rules of both I_h and D_{2h} symmetries.

The C_{20}^{+2} system has a large DFT gap (5.53 eV) which is often associated with a dominant role of the non-interacting solution in the many-body wave function. The λ_0 coefficient is expected to dominate the final optimized trial wave function. All initial coefficients λ_n of $\Psi_T(\mathbf{R})$ were set to random values, but for λ_0 which was set to zero. New λ_n values were sampled with ~ 5094 walkers every 100 DMC steps. We found that when the quality of the wave function is poor, it is better (i) to update λ_n frequently (after only 4 samplings),

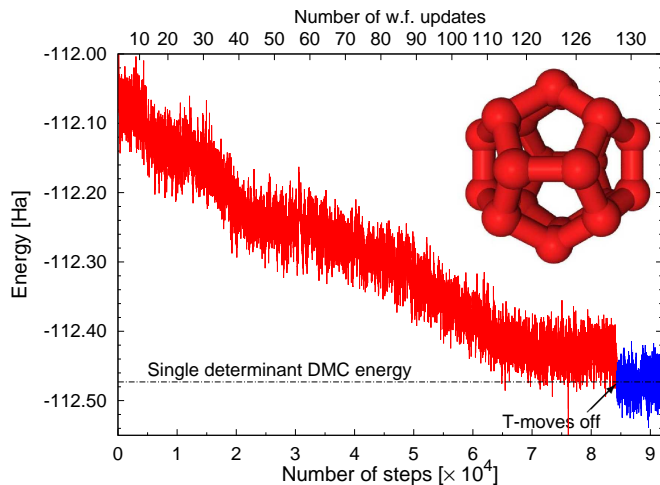


FIG. 3: Proof of principle of SHDMC for larger systems. Initial evolution of the average local energy for a SHDMC run with branching[8] generated for C_{20}^{+2} , with random initial coefficients (see text). Inset: calculated icosahedral cluster C_{20}^{+2} .

and (ii) to use the T-moves approximation [24] which limits persistent configurations. As the quality of the wave-function improved, we gradually increased the accumulation time (up to 96 samplings) and removed the T-moves approximation (which, in practice, hinders the final SHDMC convergence). Figure 3 shows that SHDMC can correct nodal errors as large as 0.5 Ha. The calculation was stopped when we obtained an energy of $-112.487(2)$ Ha compared with the single determinant energy of $-112.473(1)$ Ha. We have confidence that SHDMC can be applied to cases where the nodal structure of the ground-state is completely unknown since it is successful and converges to the expected result starting from random.

The SHDMC recursive runs required 220 hrs on 1024 processors (Cray XT4). This can be reduced to ~ 100 hrs starting from the ground state determinant. Comparable EMVMC calculations with the same basis were unsuccessful, presumably due to the statistical errors in the Hessian and overlap matrices. The energy was not improved with EMVMC ($-112.488(3)$ Ha) even selecting a basis with the largest 104 coefficients of the 694 sampled in SHDMC. The estimated running time for EMVMC with CASINO 2.5 using $N_b = 694$ and just 400 configurations [25] on 1024 processors is already ~ 100 hrs, suggesting that for C_{20}^{+2} SHDMC is faster than EMVMC. However, both methods can be improved for large N_b (e.g. as in Ref. 26), by removing redundant IO etc.

Summary — We have shown that the SHDMC wave function converges to the ground-state of our best CI calculations and is systematically improved as the number of coefficients sampled increases and the statistics are improved. SHDMC presents equivalent accuracy to the EMVMC approach [10, 11] starting from random coefficients. SHDMC is numerically robust and can be automated.

The number of independent degrees of freedom of the nodes increases exponentially with the number of elec-

trons. [9] Since EMVMC is based on VMC, the prefactor for its computational cost is much smaller than SHDMC. However, the number of quantities sampled in EMVMC is quadratic with respect to the number of degrees of freedom. In addition, EMVMC requires inverting a noisy matrix. These requirements cause EMVMC to scale at least quadratically. In contrast, SHDMC only requires one to sample a number of quantities linear in the number of optimized degrees of freedom. Therefore, a crossover between the methods is expected for systems of sufficient size or complexity. Tests on the large C_{20}^{+2} fullerene system demonstrate that SHDMC is robust and that the nodes are systematically improved even starting from a random coefficients in the trial wave function. This shows that SHDMC can be used to find the nodes of unknown complex systems of unprecedented size.

We thank D. Ceperley, R. M. Martin and C. J. Umrigar for critically reading the manuscript and useful comments. This research used computer resources supported by the U.S. DOE Office of Science under contract DE-AC02-05CH11231 (NERSC) and DE-AC05-00OR22725 (NCCS). Research sponsored by U.S. DOE BES Division of Materials Sciences & Engineering (FAR, MLT) and ORNL LDRD program (MB). The Center for Nanophase Materials Sciences research was sponsored by the U. S. DOE Division of Scientific User Facilities (PRCK). Research at LLNL was performed under U.S. DOE contract DE-AC52-07NA27344 (RQH).

-
- [1] B. L. Hammond, W. A. Lester, Jr., and P. J. Reynolds, *Monte Carlo Methods in Ab Initio Quantum Chemistry* (World Scientific, Singapore-New Jersey-London-Hong Kong, 1994).
 - [2] W. M. C. Foulkes, L. Mitas, R. J. Needs, and G. Rajagopal, *Rev. Mod. Phys.* **73**, 33 (2001).
 - [3] D. M. Ceperley, *J. Stat. Phys.* **63**, 1237 (1991).
 - [4] M. Troyer and U. J. Wiese, *Phys. Rev. Lett.* **94**, 170201 (2005).
 - [5] D. M. Ceperley and B. J. Alder, *Phys. Rev. Lett.* **45**, 566 (1980).
 - [6] J. B. Anderson, *Int. J. Quantum Chem.* **15**, 109 (1979).
 - [7] P. J. Reynolds, D. M. Ceperley, B. J. Alder, and W. A. Lester, *J. Chem. Phys.* **77**, 5593 (1982).
 - [8] F. A. Reboredo, R. Q. Hood, and P. R. C. Kent, *Phys. Rev. B* **79**, 195117 (2009).
 - [9] F. A. Reboredo, *Phys. Rev. B* **80**, 125110 (2009).
 - [10] C. J. Umrigar and C. Filippi, *Phys. Rev. Lett.* **94**, 150201 (2005).
 - [11] C. J. Umrigar, J. Toulouse, C. Filippi, S. Sorella, and R. G. Hennig, *Phys. Rev. Lett.* **98**, 110201 (2007).
 - [12] C. Umrigar (priv. commun.).
 - [13] L. Reatto, *Phys. Rev. B* **26**, 130 (1982).
 - [14] M. Burkatzki, C. Filippi, and M. Dolg, *J. Chem. Phys.* **126**, 234105 (2007).
 - [15] J. Paldus and X. Li, *Adv. Chem. Phys.* **110**, 1 (1999).
 - [16] M.W. Schmidt, et al, *J. Comput. Chem.* **14**, 1347 (1993).
 - [17] A symmetry-adapted linear combination of Slater determinants.
 - [18] L.K. Wagner, M. Bajdich, and L. Mitas, *J. Comp. Phys.* **228**, 3390 (2009).
 - [19] We included excitations up to quadruple level.
 - [20] X. Tang, Yu Hou, C. Y. Ng, and B. Ruscic, *J. Chem. Phys.*, **123**, 074330 (2005).

- [21] L. Bytautas and K. Ruedenberg, J. Chem. Phys., **122**, 154110 (2005).
- [22] R. J. Needs, M. D. Towler, N. D. Drummond, and P. López Ríos, J. Phys. Condens. Matter **22**, 023201 (2010).
- [23] L. Kronik et al. Phys. Status Solidi B **243**, 1063 (2006).
- [24] M. Casula, Phys. Rev. B **74**, 161102(R) (2006).
- [25] These configurations are not enough for $N_b = 100$.
- [26] P. K. V. V. Nukala and P. R. C. Kent, J. Chem. Phys. **130**, 204105 (2009).